Proceedings of 2017 IEEE
International Conference on Mechatronics and Automation
August 6 - 9, Takamatsu, Japan

A Hybrid Propulsion Device for the Spherical Underwater Robot (SUR III)

Shuoxin Gu[1], Shuxiang Guo[*2,*3]

[1]*Graduate School of Engineering, Kagawa University, Takamatsu, Kagawa 761-0396, Japan*

[*3]*Department of Intelligent Mechanical Systems Engineering, Kagawa University, Takamatsu, Kagawa 761-0396, Japan*

s16d642@stu.kagawa-u.ac.jp

Linshuai Zhang[1], Yi Yao[1]

[*2] *Key Laboratory of Convergence Medical Engineering and System and Healthcare Technology, the Ministry of Industry Information Technology, School of Life Science, Beijing Institute of Technology, Haidian District, Beijing 100081, China*

guo@eng.kagawa-u.ac.jp

***Abstract* - The propulsion system as the main power for the underwater robot will extremely influence its hydrodynamic performance. This paper focuses on a novel hybrid propulsion device for the third-generation spherical underwater robot (SUR III) with both vectored water-jet thrusters and propeller thrusters. To the limited space and mechanism, the hybrid propulsion device not only reserves the symmetric structure to maintain balance underwater, but also enhances the better property. And the diversity of the movement is also proposed for the different target as remote or hover. In order to analyze the hydrodynamic characteristics of the propeller, we establish the flow field with the multi-reference frame method to calculate the pressure and thrust of the propeller in ANSYS CFX. Finally, we set up the experimental system with a 6-DOFs load cell to measure the thrust of the propeller. Comparing the simulation and experiment results, the simulation thrust error is less than 8.5%. Meanwhile the power of the propeller thruster is 22.5% better than the water-jet thruster.**

Index Terms – Hybrid Propulsion Device, Spherical Underwater Robot, Hydrodynamic Characteristic, Multi-reference Frame Method, Computational Fluid Dynamics (CFD)

I. INTRODUCTION

The exploration and discovery in the unknown ocean are developed more and more quickly, the autonomous underwater vehicles (AUVs) are widely used in oceanographic research [1]-[2]. The different applications correspond to different configuration, size, propulsion methods and shape of the underwater robots. For example, a smaller, flexible and low-speed design of the robot may be reasonable for underwater applications so as to easily enter some small places [3]. MIT researchers proposed an oval-shaped submersible robot which is smaller than a football. It slides along the underwater surface with the flattened side as an ultrasound scanner [4]. And the streamlined shape is required for high-speed movements. The flow field numerical simulation of an underwater vehicle with streamlined shape was carried out. The simulation results can play a important role in the optimal design of pump jet thruster and the hydrodynamic characteristics of underwater vehicle [5]. As we know, the propulsion system plays a critical role in controlling the underwater robot. And there are various designs for propulsion device, such as propellers, poles, magneto hydrodynamic drives, sails and oars. Especially, the propeller is the most common propulsion method for the underwater robots and vehicles. Chen et al. [6] proposed a design of foldable propellers for a hybrid-driven underwater glider. The driven mode of the glider can be changed according to requirements by adjusting the statement of the propellers. And the simulation results show that the drag force can be reduced significantly when the glider is operating in the gliding mode compared with a conventional unfoldable design. Not only that, the propeller is also can be used in biomimetic underwater robots [7]-[9]. Mazumdar et al. [10] developed a new type of spherical underwater robot that uses only a single pump and two fluidic valves to achieve three dimensional motions. Lv et al. [11] developed a type of distributed pump-jet propulsion system (DPJP) with two or four specially designed pump-jet pods located around the axisymmetric underwater vehicle body symmetrically. In our previous research, a spherical underwater robot equipped with multiple vectored water jet-based thrusts was designed [12]. The evaluation simulation and experiments were carried out to verify the basic motions of a prototype robot [13]. On this basis, Yue et al. [14] described the development of the second-generation Spherical Underwater Robot (SUR-II). The hydrodynamic analysis was carried out to verify the estimated parameters such as the velocity vectors, pressure contours and drag coefficient [15]-[17]. In addition, the propulsion force obtained from the experiment verified the theoretical calculations and simulation results [14]. They also enhanced the electrical and control system of the robot [18]. In the follow-up study, a father-son underwater intervention robotic system was proposed to realize the underwater manipulation for the narrow space exploration [19]-[20]. The next development of the SUR was that Li et al. [21]-[24] proposed the third-generation spherical underwater robot (SUR III) with four water-jet thrusters. And the acoustic communication methods were also proposed for SUR III [25]. These underwater robots can provide advantages such as keeping stability and accuracy to the specific location with the

low-speed mode, improving velocity to a certain area with the high-speed mode. On the downside, the low-speed mode robot will waste a lot of time for long distance navigation, and high-speed robot close to the object with a lot of noise, and can't guarantee the accuracy of position. Therefore, it is extremely important for underwater robots to provide a mixed mode of high and low speed during ocean inspections

In this paper, a hybrid propulsion system for the spherical underwater robot was proposed. It includes two kinds of propulsion mode. One is the propeller-based mode; the other is the water-jet thruster-based mode. The propeller-based mode will be used for the long distance underwater movement with high-speed. The water jet-based mode will be adopted with low-speed in order to avoid noise and interference for hover. This kind of high and low speed hybrid propulsion mode can not only save the detection time and improve the work efficiency, but also can improve the detection precision and accuracy when slowly approaching the target.

II. Development of the Hybrid Propulsion System

A. Mechanism of the hybrid-propulsion system

The SUR III has four vectored water-jet thrusters which are homogeneously located around the robot [24]. Fig. 1 displays the top view of the previous SUR III. Although the vectored water-jet thruster has the advantage as low noise, but the propulsive thrust is limited by the space and structure. The propeller thruster is often employed in the propulsion systems for underwater robots. Its good power performance and reliability are all we need. However, the noise of the propeller is higher than the vectored water-jet thruster. Therefore, a hybrid motion system is proposed to improve the hydrodynamic thrust of the SUR III in the restricted space and structure. In the underwater mission, using the propeller propulsion mode quickly and effectively close to the target, then switch the water-jet propulsion mode to reduce the noise near the target.

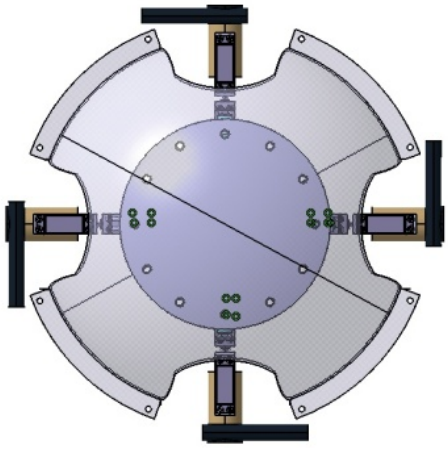

Fig. 1 Previous Design of the SURIII

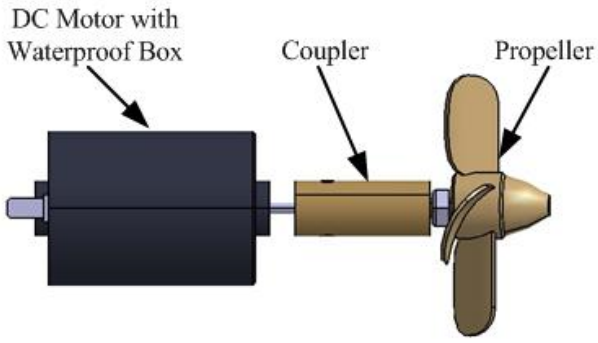

Fig. 2 3D Model of the Propeller Thruster

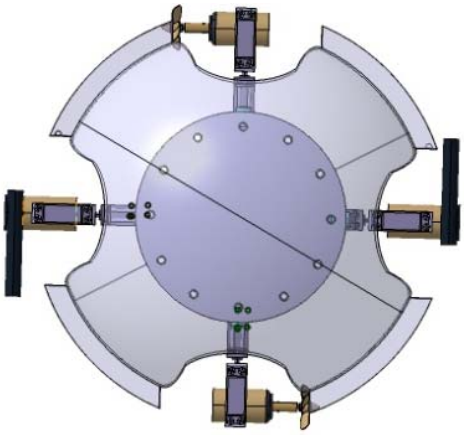

Fig. 3 Revised Design of the SUR III

In the previous research, it verified that the structure of the water-jet thruster is stable and reliable. Based on this we will keep the basic mechanism of the water-jet thruster to cooperate the propeller thruster. The DC motor can reach 400 revolutions per minute. In order to connect the DC motor and the propeller, a coupling mechanism is designed. One side of the coupler is fixed with the DC motor by jackscrew, and on the other side is projected as the screw to joint with propeller. The mechanism of the propeller thruster is shown in Fig. 2. Considering about the symmetrical structure of the robot, two opposite water-jet thrusters were reserved and the other two were replaced by the propeller thruster. The new revised mechanical construction is shown in Fig. 3.

B. Motion state of the revised SURIII

There are four DOFs which included surge, sway, heave and yaw in SUR III. The surge and sway are the movement in the same plane. Thus, we will focus on three DOFs which are surge, heave and yaw. In surge motion, the hybrid motion of two propellers and one vectored water-jet thruster is regarded as the high-speed mode, and the motion of two vectored water-jet thruster can be regarded as the low-speed mode, these two kinds of motions are shown in Fig. 4(a) and Fig. 4(b). In addition, other motions all belong to the middle-speed mode. In yaw motion, the rotation angle can be measured by the gyroscope. If all thrusters work at the same time, the robot

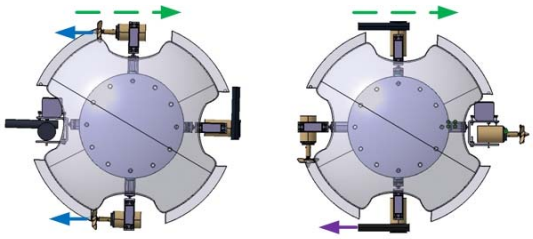

(a) High-speed in Surge Motion (b) Low-speed in Surge Motion

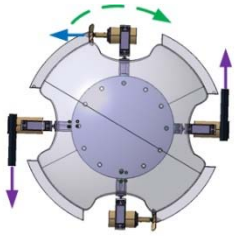

(c) Yaw Motion

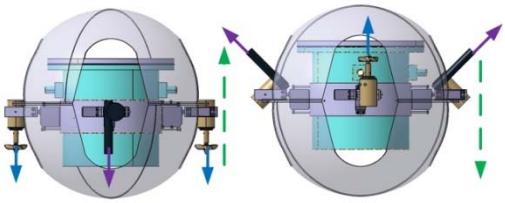

(d) Up Motion (e) Down Motion

Thrust of the Water-jet Thruster

Thrust of the Propeller Thruster

Direction of the Motion

Fig. 4 Motion State of the Revised SUR III

can be realized a high-speed rotating mode which is shown in Fig. 4(c), this style is suitable for fast turning requirement. Otherwise working of two opposite vectored water-jet thrusters will realize a low-speed rotating mode. Due to the low speed, it is easier to control, so it can receive an accuracy rotation. Final one is the heave motion which involved two kinds of motion: up and down, corresponding to Fig. 4(d) and Fig. 4(e).

III CFD Simulation of the Propeller

A. Dynamic analysis

The details of how the propeller generates thrust are very complex, but we can still learn a few of the fundamentals using the simplified momentum theory presented here. Fig. 5 shows a schematic of a propeller propulsion system. In this schematic, the spinning propeller is assumed as a disk and surrounded by water. When it works, there is an abrupt change in pressure across the disk. We use the ΔP to express the changed pressure. Turning to the math, the thrust F_T equals to,

$$F_T = \Delta P * A \tag{1}$$

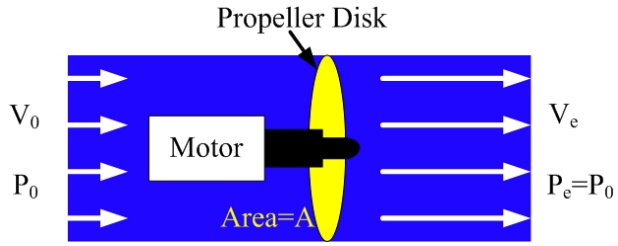

Fig. 5 Schematic of the Propeller Propulsion

Table I
Parameters of the Propeller

List of items	value
Propeller diameter, D	0.05m
Hub/propeller diameter ratio, dh/D	0.2
Number of blades, N_b	4

where A is the area of the propeller disk. And the changed pressure can be calculated by the subtraction between the pressure ahead and behind the propeller disk.

$$\Delta P = P_{te} - P_{t0} \tag{2}$$

In this research, the viscosity can be ignored and we do not consider about the compressed fluid either. Therefore, the Bernoulli's equation can be used to relate the pressure and velocity of the upstream and downstream. The total pressure of upstream and downstream are as follow,

$$P_{t0} = P_0 + 0.5\rho {V_0}^2 \tag{3}$$

$$P_{te} = P_0 + 0.5\rho {V_e}^2 \tag{4}$$

where P_0 is the static pressure, V_0 is the velocity of the robot, and V_e is exit velocity of the propeller. According to the above equations, finally the thrust can be obtained as,

$$F_T = 0.5\rho A({V_e}^2 - {V_0}^2) \tag{5}$$

B. Pre-processing for the CFD simulation

The 3D model of propeller is established in CATIA. And the parameters of the propeller are given in Table 1. Based on the multi-reference frame method, the fluid model included the station domain, rotation domain and propeller. Both of the station and rotation fluid fields were assumed as the cylinder. Fig. 6(a) illustrates the overall plot of the fluid model. With the length and diameter of the cylinder can define the boundary of the domains. The rotation domain boundary is 0.5D for length and 1.2D for diameter, and the station domain is 10D for length and 5D for diameter. The rotating speed of the propeller is set to 400rev/min. The inflow velocity of the station domain is 0.3m/s. The station and rotation domain are connected by the interfaces which is shown in Fig. 6(b).

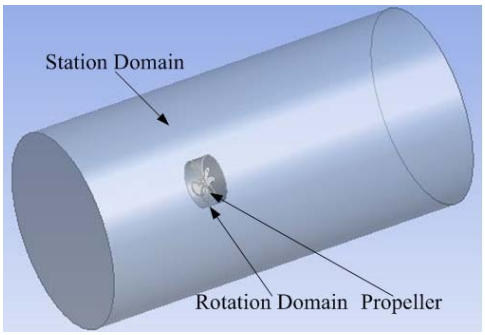

(a) Overall Plot of the Fluid Model

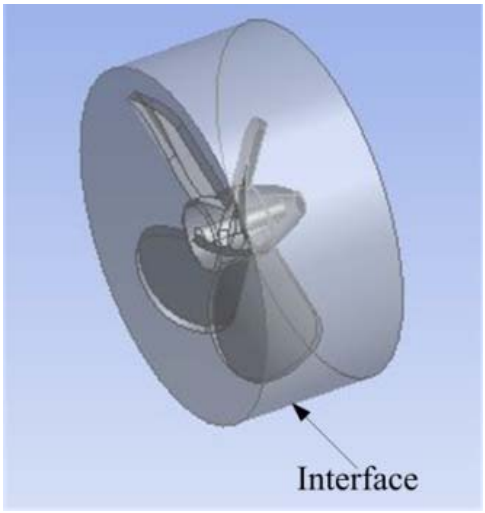

(b) Rotation Domain

Fig. 6 Fluid Model of the Propeller

C. *Post-processing for the CFD simulation*

According to the results in the CFX post-processing, the pressure distribution of the blade surfaces can be analyzed in Fig. 7. On the one hand, Fig. 7(a) shows the pressure surface, the pressure increases from the root to the top of the blade, and the maximum pressure roughly occurs in the 0.6R, then the pressure gradually reduces and at the top reaches the minimum. On the other hand, Fig. 7(b) shows the suction surface, the pressure in the middle of the suction surface is the minimum, and it increases to the leading edge and trailing edge. Simultaneously, we also obtain the exit velocity of the propeller which equals to 1.68m/s, and the flow velocity of the station domain can be regarded as the velocity of the robot. Hence, the thrust force will be calculated by equation (5), and F_T=2.68N in this situation.

IV Experimental Results

In order to verify the performance of the propeller firstly, an experiment was implemented. In this experiment, a load cell with six-DOFs was made use of measuring the propulsive thrust of the propeller. We built a set of experimental system to complete the test. The overall system and the coordinate system of the load cell is shown in Fig. 8. A steel bar was fixed with both of the load cell and propeller thruster, so that

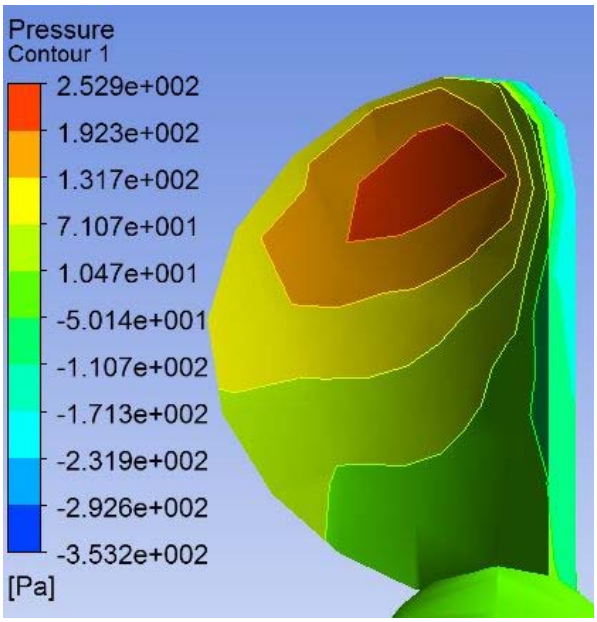

(a) Pressure Surface

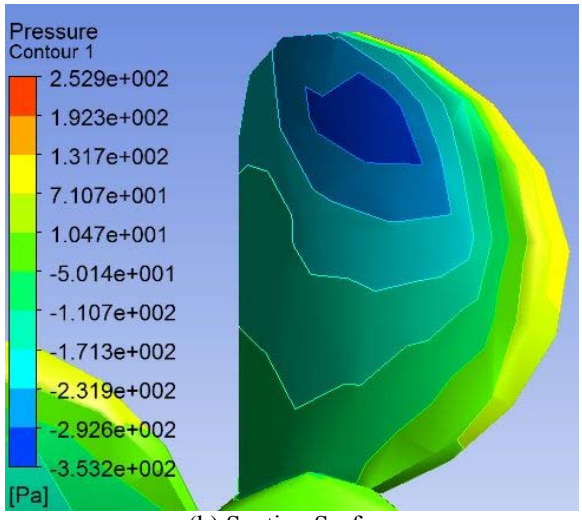

(b) Suction Surface

Fig.7 Pressure Contour of the Blade

the propulsive thrust will occur in the XY plane. And put the propeller thruster in the water. Since the steel bar and the load cell are the rigid bodies, the propeller thruster won't produce the relative displacement in the XY plane by the deformation of the experimental device. We can assume the force in the Y axis as the propulsive thrust.

For setting the initial parameter before the experiment, first we measured the force and torque in each direction when the experimental device is completely stationary. We tested for ten times and each time can get 120 values, then calculated the average experimental values to program the initial value of 0 in each direction for the stationary device. Afterwards the propeller thruster is energized by the DC generator. For the objective experimental results, we conduct ten cycles of test and every test will obtain 120 test values in each direction.

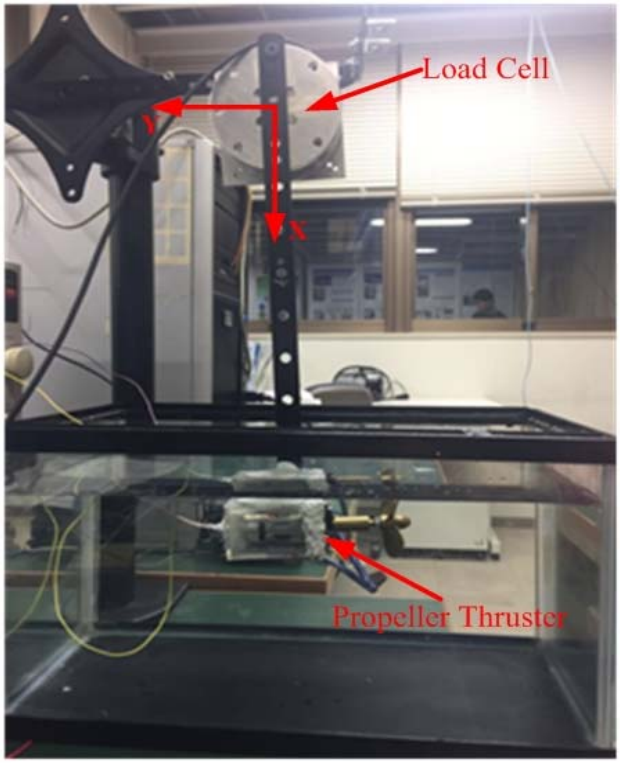

Fig.8 Experimental System

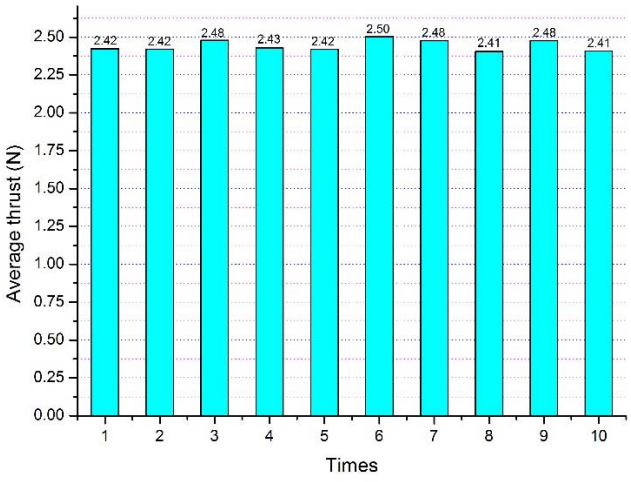

Fig.9 Average Thrust of Each Time Test

The experimental results are consistent with our assumptions. The test forces in X and Z axis are very small and can be ignored. Therefore, the force in Y axis is the experimental thrust of the propeller. Fig. 9 is the average thrust for each test. And the final average value of the thrust is 2.45N, which indicates an 8.5% error compared to the calculated value. Therefore, the results of the CFD simulation are acceptable. Meanwhile, the experiment result for the thruster of the propeller reveals that the power of propeller is 22.5% stronger than the water-jet thruster.

V Conclusion and Future Work

This paper presented a hybrid propulsion device for the third-generation spherical underwater robot (SUR III). First of all, the mechanism of the hybrid-propulsion device was proposed. Due to the better power performance of the propeller thruster and the low noise of the water-jet thruster, this novel hybrid-propulsion system both can approach the target in a high speed and undertake in a low speed to avoid noise and collision. After that, in order to figure out the thrust of the propeller, some fundamentals using the simplified momentum theory were proposed. And a CFD simulation with the multi-reference frame method was also carried out. We also got a theoretical value of the thrust for the propeller. Finally, an experiment was conducted by using a 6-DOFs load cell. The experiment results illustrated that the thrust error is fewer than 8.5% with the result of CFD simulation. Moreover, the thrust of propeller is 22.5% higher than before.

In the future, we will focus on the experiment of the whole propulsion system and the robot underwater.

Acknowledgment

This research is partly supported by National Natural Science Foundation of China (61375094), National High Tech. Research and Development Program of China (No.2015AA043202), and SPS KAKENHI Grant Number 15K2120.

References

[1] C. Eriksen, T. James-Osse, R. Light, T. Lehman, P. Sabin, J. Ballard, A. Chiodi, “Seaglider: A Long-Range Autonomous Underwater Vehicle for Oceanographic Research”, IEEE Journal of Oceanic Engineering, vol. 26, no. 4, pp. 424-436, 2001.

[2] B. Claus, R. Bachmayer, L. Cooney, “Analysis and Development of a Buoyancy Pitch based Depth Control Algorithm for a Hybrid Underwater Glider”, Proceedings of the 2012 IEEE/OES Autonomous Underwater Vehicles (AUV), pp. 1-6, United Kingdom, 2012.

[3] X. Lin, S. Guo, C. Yue and J. Du, “3D Modelling of a Vectored Water Jet-Based Multi-Propeller Propulsion System for a Spherical Underwater Robot”, International Journal of Advanced Robotic Systems, vol.10, no. 1, pp. 1-8, 2013.

[4] https://robotics.mit.edu/underwater-robot-port-security

[5] Y. Dong, X. Duan, S. Feng, Z. Shao, “Numerical Simulation of the Overall Flow Field for Underwater Vehicle with Pump Jet Thruster”, Procedia Engineering, vol. 31, pp. 769-774, 2012.

[6] Z. Chen, J. Yu, A. Zhang, F. Zhang, “Design and Analysis of Folding Propulsion Mechanism for Hybrid-driven Underwater Gliders”, Ocean Engineering, vol. 119, pp. 125-134, 2016.

[7] Q. Pan, S. Guo, T. Okada, “A Novel Hybrid Wireless Microrobot”, International Journal of Mechatronics and Automation, vol. 1, no. 1, pp. 60-69, 2011.

[8] B. Gao, S. Guo, X. Ye, “Motion-control Analysis of ICPF-actuated Underwater Biomimetic Microrobots”, International Journal of Mechatronics and Automation, vol. 1, no. 2, pp. 79-89, 2011.

[9] D. Scaradozzi, G. Palmieri, D. Costa, A. Pinelli, “BCF Swimming Locomotion for Autonomous Underwater Robots: A Review and a Novel Solution to Improve Control and Efficiency”, Ocean Engineering, vol. 130, pp. 437-453, 2017.

[10] A. Mazumdar, A. Fittery, W. Ubellacker, and H. Asada, “A Ball-Shaped Underwater Robot for Direct Inspection of Nuclear Reactor and Other Water-filled Infrastructure”, Proceedings of 2013 IEEE International Conference on Robotics and Automation, pp. 3415-3422, Germany, 2013.

[11] X. Lv, Q. Zhou, B. Fang, “Hydrodynamic Performance of Distributed Pump-jet Propulsion System for Underwater Vehicle”, Journal of Hydrodynamics, vol. 26, no. 4, pp. 523-530, 2014.
[12] X. Lin, S. Guo, “Development of a Spherical Underwater Robot Equipped with Multiple Vectored Water-Jet-Based Thrusters”, Journal of Intelligent & Robotic Systems, vol. 67, no. 3, pp. 307-321, 2012.
[13] X. Lin, S. Guo, K. Tanaka, S. Hata, “Underwater Experiments of a Water-jet-based Spherical Underwater Robot”, Proceedings of the 2011 IEEE International Conference on Mechatronics and Automation, pp. 738-742, China, 2011.
[14] C. Yue, S. Guo, M. Li, Y. Li, H. Hirata, H. Ishihara, “Mechatronic System and Experiments of a Spherical Underwater Robot: SUR-II”, Journal of Intelligent & Robotic Systems, vol. 80, no. 2, pp. 325-340, 2015.
[15] C. Yue, S. Guo, X. Lin, J. Du, “Analysis and Improvement of the Water-jet Propulsion System of a Spherical Underwater Robot”, Proceedings of 2012 IEEE International Conference on Mechatronics and Automation, pp. 2208-2213, China, 2012.
[16] C. Yue, S. Guo, and L. Shi, “Hydrodynamic Analysis of the Spherical Underwater Robot SUR-II”, International Journal of Advanced Robotic Systems, vol. 10, no. 247, pp. 1-12, 2013.
[17] C. Yue, S. Guo, M. Li, “ANSYS FLUENT-based Modeling and Hydrodynamic Analysis for a Spherical Underwater Robot”, Proceedings of the 2013 IEEE International Conference on Mechatronics and Automation, pp. 1577-1581, Japan, 2013.
[18] S. Guo, J. Du, X. Lin, C. Yue, “Adaptive Fuzzy Sliding Mode Control for Spherical Underwater Robots”, Proceedings of 2012 IEEE International Conference on Mechatronics and Automation, pp. 1681-1685, China, 2012.
[19] C. Yue, S. Guo, Y. Li, M. Li, “Bio-Inspired Robot Launching System for a Mother-Son Underwater Manipulation Task”, Proceedings of 2014 IEEE International Conference on Mechatronics and Automation, pp. 174-179, China, 2014.
[20] C. Yue, S. Guo, L. Shi, “Design and Performance Evaluation of a Biomimetic Microrobot for the Father-son Underwater Intervention Robotic System”, Microsystem Technologies, vol. 22, no. 4, pp. 831-840, 2015.
[21] Y. Li, S. Guo, C. Yue, “Preliminary Concept and Kinematics Simulation of a Novel Spherical Underwater Robot”, Proceedings of 2014 IEEE International Conference on Mechatronics and Automation, pp. 1907-1912, China, 2014.
[22] Y. Li, S. Guo, C. Yue, “Study on the Control System of a Novel Spherical Underwater Robot”, Proceedings of 2015 IEEE International Conference on Mechatronics and Automation, pp. 2100-2105, China, 2015.
[23] Y. Li, S. Guo, C. Yue, “Preliminary Concept of a Novel Spherical Underwater Robot”, International Journal of Mechatronics and Automation, vol. 5, no. 1, pp. 11-21, 2015.
[24] Y. Li, S. Guo, Y. Wang, “Design and Characteristics Evaluation of a Novel Spherical Underwater Robot”, Robotics and Autonomous Systems, vol. 94, pp. 61-74, 2017.
[25] Y. Li, S. Guo, “Communication between Spherical Underwater Robots Based on the Acoustic Communication Methods”, Proceedings of 2016 IEEE International Conference on Mechatronics and Automation, pp. 403-408, China, 2016.